Individual- versus group-optimality in the production of secreted bacterial compounds

Konstanze T. Schiessl[1,2,†] , Adin Ross-Gillespie[3], Daniel M. Cornforth[4], Michael Weigert[3], Colette Bigosch[1], Sam P. Brown[5], Martin Ackermann[1,2,*], Rolf Kümmerli[1,3,*]

* contributed equally
[†] Current address: Department of Biological Sciences, Columbia University, 1212 Amsterdam Avenue, New York, NY 10027, USA.

1 Department of Environmental Microbiology, Swiss Federal Institute of Aquatic Science and Technology (Eawag), Überlandstrasse 133, 8600 Dübendorf, Switzerland.

2 Department of Environmental Systems Science, Swiss Federal Institute of Technology (ETH Zurich), Universitätsstrasse 16, 8092 Zürich, Switzerland.

3 Department of Plant and Microbial Biology, University of Zürich, Winterthurerstrasse 190, 8057 Zürich, Switzerland.

4 Department of Molecular Biosciences, University of Texas, 2500 Speedway, Austin, USA.

5 Institute of Evolutionary Biology and Centre for Immunity, Infection and Evolution, University of Edinburgh, West Mains Road, Ashworth Laboratories, Edinburgh EH9 3JT, UK

Abstract

How unicellular organisms optimize the production of compounds (enzymes and metabolites) is a fundamental biological question. While it is typically thought that this production is optimized at the individual cell level, we examine whether it can also be optimized at the group level instead, through specialization, where a fraction of cells secretes and shares compounds with the other group members. Using mathematical modeling, we show that within-group division of labor is promoted if (1) the per-compound production costs diminish with higher production volumes, and (2) compound sharing is sufficiently high. Experiments with pyoverdine, a shareable compound secreted by *Pseudomonas aeruginosa*, indeed revealed diminishing costs, yet instead of dividing labor, all cells engage in pyoverdine production. We conclude that even when diminishing costs ostensibly favor phenotypic specialization, its evolution can either be hindered by factors limiting reliable compound sharing in the natural environment or mechanistic constraints impeding stochastic or signal-induced heterogeneity to arise. Thus, shifts in the level of selection, from individuals to groups, might be restricted in loose microbial groups.

Introduction

Production of proteins and metabolites is at the basis of many cellular processes. Because of its fundamental importance, there has been much interest in understanding the mechanisms that control compound production at the cellular

level (Dekel and Alon 2005; Shachrai et al. 2010; Eames and Kortemme 2012; Price et al. 2013). The general consensus is that there should be a production optimum, at which the net benefit of producing a specific compound (protein or metabolite) peaks. Moving away from that optimum either results in wasteful overproduction or insufficient compound supply. Indeed, experimental work has demonstrated that populations of unicellular organisms evolve towards such optima in laboratory settings (Dekel and Alon 2005; Poelwijk et al. 2011).

One implicit assumption of the above-mentioned work on unicellular organisms is that optimality is achieved at the level of the individual. This means that every individual in a population is expected to tune its compound expression level to the same optimum. However, bacteria and other microbes are not solitary organisms, but often live in dense social groups, where they can interact and communicate with one another. This opens the possibility for optimality in compound production to arise at the level of the clonal group and not the individual. Indeed, recent experimental studies report cases of bimodal expression patterns across individuals in clonal groups, which could reflect group-level optimization (Diard et al. 2013; van Gestel et al. 2015). Here, we formally ask whether group optimality in compound production is indeed possible and examine the conditions required for natural selection to shift optimization foci from the individual- to the group level (i.e. representing a change in the level of selection, where clonal groups emerge as a new functional unit). Following the logic of (Frank 2013), we propose that

heterogeneous expression profiles could be particularly common for secreted extra-cellular compounds. The reasoning is that secreted compounds, including enzymes and secondary metabolites, can be shared at the level of the clonal group, thereby decoupling individual expression levels from fitness returns. In other words, the benefit an individual gains from the production of a shared compound is determined not by the individual's own investment, but by the production level of the entire group (Frank 2013). This could potentially trigger the evolution of a group-optimal strategy, characterized by a type of division of labor where the clonal group splits into phenotypic producers and nonproducers. This split could be mechanistically implemented either by intrinsic or extrinsic (signal-induced) bistable expression of the relevant synthesis genes (Dubnau and Losick 2006; Veening et al. 2008; Ackermann et al. 2008; West and Cooper 2016).

We argue that secreted compounds must meet two requirements for such a division of labor to evolve, and we investigate these using mathematical modeling and experiments with bacteria. Our first prediction is that specialization into producers and non-producers can be favored when the per-unit production costs diminish with higher compound production volumes, following the principle of economies of scale. This economic principle states that, if production costs are diminishing and products are shared, net benefits are maximized if only few individuals engage in production. By producing large quantities, these specialists distribute the initial fixed costs over many units of output (Case et al. 2011).

Diminishing costs seem likely for the production of numerous secreted secondary metabolites (including antibiotics, toxins, surfactants, siderophores) whose synthesis requires dedicated cellular machinery. One important example are peptides produced via nonribosomal peptide synthesis instead of ribosomal synthesis (Caboche et al. 2007; Miethke and Marahiel 2007). Nonribosomal peptide synthesis requires the buildup of complex synthesis machineries prior to metabolite production. Thus, one would predict that, following an initially high investment of resources to set up this nonribosomal assembly line, the costs of actually using it for compound production should be comparatively low. The more it is used, the lower are the overall costs per unit of the final product. This situation should favor a division of labor, where some cells in a population specialize in compound production, whereas others do not produce it at all.

Our second prediction is that a high shareability of the secreted compound among clone mates must be guaranteed for division of labor to evolve. This is because phenotypic non-producers fully depend on the compound provisioning from the surrounding producing cells. While high shareability has been demonstrated for numerous secreted bacterial compounds under laboratory settings (Griffin et al. 2004; Diggle et al. 2007; Xavier et al. 2011), we still know little about the extent of metabolite sharing in the natural environment, where a number of biotic and abiotic factors are expected to play a role. For instance, while shareability is typically high in dense clonal groups (Kümmerli et al. 2009a; Julou et al. 2013; Olejarz and

Nowak 2014), it can be reduced at low cell density (Ross-Gillespie et al. 2009; Sanchez and Gore 2013; van Gestel et al. 2014; Scholz and Greenberg 2015) where compounds are easily lost due to diffusion and thereby do not reach designated recipients (Kümmerli et al. 2014). Another complication might be that natural communities are rarely clonal and efficient compound diffusion and thereby sharing might be hindered by the sheer presence of other species (Inglis et al. 2016) or by 'cheating' genotypes that take up the compound but have lost the ability to produce it (Griffin et al. 2004; Cordero et al. 2012).

We tested our predictions combining empirical experiments with mathematical modeling. As our experimental model system, we used the production of pyoverdine, a siderophore synthesized via nonribosomal peptide synthetases, and secreted by the bacterium *Pseudomonas aeruginosa* to scavenge iron from the environment (Visca et al. 2007). Pyoverdine can be shared among clonal bacteria (Meyer et al. 1997; De Vos et al. 2001; Griffin et al. 2004). We first measured costs and benefits of pyoverdine production to test whether an economies of scales pattern (i.e. a diminishing production cost function) applies to pyoverdine. We then used mathematical modeling to investigate how cost and benefit functions interact and shape the net benefit of individuals as a function of the level of division of labor and compound shareability. Finally, we combined automated flow cytometry with single-cell microscopy to quantify single-cell pyoverdine expression profiles, and

to test whether production of pyoverdine is optimized at the individual- or at the group-level.

Material and Methods

Strains

All our experiments were carried out with the clinical isolate *P. aeruginosa* PAO1 (ATCC 15692), the most widely studied strain of this species. To measure costs and benefits of pyoverdine production, we constructed the conditional pyoverdine mutant PAO1-*pvdSi*, where we put the production of pyoverdine under the control of the IPTG inducible promoter P_{tac}. Specifically, we replaced the native promoter of *pvdS*, the gene coding for the iron starvation sigma factor PvdS, which controls the expression of genes coding for enzymes involved in nonribosomal peptide synthesis of siderophores. We PCR-amplified the flanking regions (FR1 upstream: 836 bp; and FR2 downstream: 987 bp) of the native *pvdS* promoter using the following set of primers (FR1F: 5'- ggg ata cac cgg aga gga ata -3', FR1R: 5' - ttt gcc att ctc acc gga ttt gat gga ggg gag aaa ttc tt -3' / FR2F-SacI: 5' - gcg cga gct cat gtc gga aca act gtc tac ccg -3', FR2R- KpnI: 5' – gcg cgg tac cat cca tat gcc cgc tgc gac a - 3'). FR2 features two restriction sites (SacI and KpnI), which we used to clone this fragment into the pME6032 vector featuring the P_{tac} promoter and *lacI* (repressor of P_{tac}). We then PCR-amplified the *lacI* - P_{tac} - FR2 construct using the primers ampF (5'- aat ccg gtg aga atg gca aa -3') and ampR (5'- tcc gag gcc tcg aga tct at -3'), and subsequently carried out fusion PCR with this amplicon

and FR1, which features a 20 bp overhang (see FR1R) reverse complementary to the *lacI* sequence. Fusion PCR included a first set of cycles, where the *lacI* - P_{tac} - FR2 amplicon and FR1 could hybridize via the overhang in the absence of primers, and therefore mutually serve each other as template and primer. During a second set of cycles, the final construct of 3242 bp length was amplified using the primers FR1 and ampR. This fragment was ligated into pGEM-T easy (A1360, Promega) for storage, and cloned into pME3087, a suicide vector, which we transformed into the *Escherichia coli* S17-1 donor strain. We then carried out mating between the S17-1 donor and the PAO1 recipient. Single crossovers were selected on LB agar supplemented with tetracycline (100 μg/ml to select against wildtype PAO1) and chloramphenicol (10 μg/ml to select against S17-1). We grew one single crossover colony overnight in LB at 37°C, during which double crossovers can occur (either reverting back to wildtype or replacing the native *pvdS* promoter with our inducible construct). To enrich for double crossovers, we added tetracycline (20 μg/ml, a bacteriostatic concentration at which non-tetracycline resistant strains stop growing). Subsequently, we added carbenicillin (2000 μg/ml) to selectively kill the growing tetracycline-resistant single crossovers. After cell washing and plating, we picked ~100 colonies from LB plates and screened for conditional pyoverdine mutants, using IPTG-induction assays and sequencing of the *pvdS* promoter site.

To investigate heterogeneity in pyoverdine expression, we used PAO1*pvdA-gfp*, a transcriptional reporter (chromosomal insertion: *att*B::*pvdA-gfp*), which links transcription of *egfp* to the transcription of *pvdA*, one of the pyoverdine

biosynthesis genes (Kaneko et al. 2007). As negative control (i.e. no GFP expression), we used the wildtype PAO1 strain obtained from Pierre Cornelis' laboratory (Ghysels et al. 2004). As positive control, we used a constitutive GFP expressing derivate of PAO1 (PAO1-*gfp*, chromosomal insertion: *att*Tn7:: P_{tac} -*gfp*) (Lambertsen et al. 2004). Finally, we generated the double-reporter strain PAO1-*mcherry-pvdA-gfp* by integrating the constitutive promoter P_{tac} linked to mcherry (*att*Tn7:: P_{tac} -*mcherry*) into PAO1*pvdA-gfp* using the miniTn7 system (Choi and Schweizer 2006).

Media and growth conditions

All experiments were carried out in casamino acids medium (CAA) containing: 5 gl^{-1} casamino acids (Merck, Switzerland), 1.18 g l^{-1} $K_2HPO_4*3H_2O$, 0.25 g l^{-1} $MgSO_4*7H_2O$, and 5.96 g HEPES (all from Sigma-Aldrich). To measure the cost of pyoverdine production, we grew our conditional pyoverdine mutant PAO1-*pvdSi* in CAA medium supplemented with 100 μM $FeCl_3$. Under these conditions, pyoverdine is not required for growth, and consequently we expect that IPTG-induced pyoverdine production will reduce bacterial growth. Thus, the cost c of pyoverdine production at a given induction level i can be measured as $c = \mu_0 - \mu_i$, where μ_0 and μ_i are the maximal growth rates of the non-induced and induced PAO1-*pvdSi* cultures, respectively. We measured the c for 10 induction levels (IPTG in mM: 0.1, 0.125, 0.15, 0.175, 0.2, 0.25, 0.3, 0.5, 1, 10) in 8-fold replication each. Induction experiments were carried out in 96-well plates, where we added

approximately 10^5 cells from an overnight LB culture to 200 μl medium. Plates were incubated in a multimode plate reader (Synergy Mx, Biotek, Switzerland) at 37°C for 24 hours. Culture growth was measured as optical density (OD; absorbance at 600 nm) at 15 minutes intervals. Cultures were shaken for 10 minutes prior to readings. Growth curves were fitted to OD trajectories from 0 to 16 hours of growth in R 3.1.1 (R Core Team (2015). R: A language and environment for statistical computing. R Foundation for Statistical Computing, Vienna, Austria. https://www.R-project.org/) using functions from the 'grofit' package (Kahm et al. 2010). In addition to OD, we also quantified the production of pyoverdine over time for each IPTG induction level. Pyoverdine is a naturally fluorescent molecule, which can be quantified through excitation at 400 nm and emission at 460 nm (Kümmerli et al. 2009b). It was previously shown that relative pyoverdine fluorescence correlates linearly with the absolute pyoverdine content in bacterial cultures (Dumas et al. 2013).

To measure the benefit of pyoverdine production, we grew PAO1-*pvdSi* in iron-limited CAA medium (using 100 mg ml^{-1} human-apo transferrin to bind iron and 20mM $NaHCO_3$ as cofactor, both from Sigma-Aldrich, Switzerland), supplemented with various amounts of purified pyoverdine (pyoverdine concentration in μM: 0, 5, 10, 25, 50, 100, 200, 400, 600, 800; in 6-fold replication each). Pyoverdine was extracted using the protocol described in (Dumas et al. 2013), and supplemented in four time intervals (after 2, 4, 6, and 8 hours of growth) to mimic the continuously

increasing pyoverdine concentrations typically observed in growing cultures. Since PAO1-*pvdSi* was not induced with IPTG in these experiments, growth was entirely dependent on the supplemented pyoverdine. Accordingly, the benefit b of pyoverdine can be measured as $b = \mu_s - \mu_0$, where μ_0 and μ_s are the maximal growth rates of the unsupplemented and supplemented PAO1-*pvdSi* cultures, respectively. Measuring growth kinetics and analysing growth curves were carried out as described above.

To quantify cell-to-cell variation in pyoverdine expression, we used a slightly modified version of the iron-limited CAA medium: 5 g Casein Hydrolysate (Merck), 0.25 g $MgSO_4*7H_2O$ (Sigma-Aldrich), 0.9 g K_2HPO_4 (Sigma-Aldrich), and 5.96 g HEPES (Sigma-Aldrich). The pH was adjusted to 7 with 5M NaOH. After autoclaving, the medium was filtered through a 0.1 µm-filter in order to remove particulate iron as well as background hindering the flow cytometry measurements (Cellulose Nitrate Membranes, 0.1 µm, 47 mm ø, Whatman). Iron availability was adjusted by addition of varying amounts of Fe(III)EDTA (Ethylenediaminetetraacetic acid Iron(III)-Sodium Hydrate, Sigma-Aldrich). In order to standardize EDTA concentrations across samples, iron-free EDTA (Ethylenediaminetetraacetic acid disodium salt dehydrate, Sigma-Aldrich) was added to reach a total EDTA concentration of 20 µM. Four iron limitation environments were tested: 0 µM, 1 µM, 5 µM and 20 µM Fe(III)EDTA. EDTA and

Fe(III)EDTA were dissolved in nanopure water, filtered through a 0.1 µm filter, and added to CAA after autoclaving.

For flow cytometry and microscopy studies, the strains were streaked from a frozen stock on LB agar and incubated overnight. Single colonies were picked and inoculated in 5 ml LB and incubated at 37°C in an orbital shaker (220 rpm). After 16 hours of incubation, the culture was diluted 1:200 in 5 ml LB and regrown to the exponential phase, corresponding to an optical density of approximately 0.13. To start the experiment, all strains were diluted 1:2000 to reach a starting cell concentration of around 10^4 cells/ml, and inoculated in 100 ml CAA. Cells were cultured in 100 ml-Schott bottles in a water bath at 37°C, oxygenated via stirring on a magnetic plate. The lid was removed and the bottles were covered with aluminum foil to allow the cultures access to oxygen. From these cultures, samples for flow cytometry and microscopy were taken.

Automated flow cytometry

We used automated flow cytometry to monitor temporal changes in the distributions of *pvdA*-reporter-associated fluorescence in cultures of *P. aeruginosa* growing under different levels of iron limitation. Our setup, broadly similar to that of (Besmer et al. 2014), enabled us to quantify the GFP fluorescent signal in a time-resolved manner. To the intake port of a C6 flow cytometer (BD Accuri, San Jose CA, USA), we fitted an electronically-controlled relay valve that allowed switching

between multiple sources. This setup permitted automated time-series sampling from up to 8 cultures in parallel. GFP-signal was detected using a 488 nm laser for excitation, and an emission detector fitted with a 533±30 nm bandpass filter. Forward- and side-scattered light produced by the 488 nm laser was also quantified, and all particles associated with a forward scatter signal of < 10000 fluorescence units were excluded *a priori* from further analysis on the basis that they were unlikely to represent intact bacterial cells. At each sampling point, the flow cytometer processed the sample at a rate of 66 µl min^{-1} for two minutes, although we retained data only from the final 20 seconds of each run, where the signal was most stable. Between each successive sample, the line was washed with 0.2% hypochlorite and nanopure water to avoid contamination and signal bleed-through. Cultures were sampled at 33-minute intervals during a total period of 180 minutes. The reporter strain, PAO1*pvdA-gfp* was tested in four different Fe-limitation environments (CAA supplemented with 0 µM, 1 µM, 5 µM and 20 µM Fe(III)EDTA, respectively). We replicated the time-series experiment 8 times, where each block included the reporter strain in all four environments, a blank control (i.e. CAA medium only), a negative control for background GFP-fluorescence (i.e. PAO1 growing in unsupplemented CAA) and two positive controls (PAO1-*gfp*, under varying levels of iron limitation). Our raw flow cytometry data likely included noise – i.e. measurements from particles that were not single, intact bacterial cells. Therefore, for each sample at each time point, we calculated 95% contours of highest posterior density for the two-dimensional space of GFP-

signal versus side scatter, and we excluded from further analyses any points lying outside these contours. These analyses, and all others described below, were performed in R 3.1.1 (R Core Team (2015). R: A language and environment for statistical computing. R Foundation for Statistical Computing, Vienna, Austria. https://www.R-project.org/).

Microscopy

In order to collect single-cell data on pyoverdine expression, we acquired snapshots of bacterial cultures with an epifluorescence microscope. Bacteria were grown in conditions identical to the flow cytometry experiments, but only measured once every hour and only tested in CAA with 20 μM EDTA, without addition of iron. At t=0h, cells were sampled directly from the LB medium. At 1, 2, and 3 hours cells were taken from the iron-limited medium and concentrated by centrifugation of 15 ml culture at 4°C, 5000 rpm, 10 minutes. Cells were kept on ice until the measurement and processed within 45 minutes.

For data acquisition, 1 μl of cell suspension was spotted on a CAA 1.5% agarose pad and covered with a cavity slide as described in (Bergmiller et al. 2011). We used an inverted fluorescence microscope (Olympus IX81) with an X-Cite 120PV fluorescence lamp (Lumen Dynamics Group Inc., Canada) and an automated stage. Pictures were acquired with a cooled CCD camera (Olympus XM10) and an UPLFLN 100xO2PH/1.3 phase contrast oil immersion objective (Olympus). Phase

contrast images were acquired with an exposure time of 20 ms, fluorescence images with an exposure time of 500 ms for gfp and 800 ms for mcherry. The filter for recording the GFP signal had the following parameters: excitation range 450-490, emission range 500-550 nm, DM 495 nm (AHF Analysentechnik, Tübingen, Germany; Article No. F46-002), the filter for mcherry: excitation range 540-580, emission range 595-665, DM 585 (AHF Analysentechnik, Tübingen, Germany; Article No. F46-008). Data for each type of experiment were recorded within one week in order to minimize variation of lamp intensity between experiments.

Growth potential of the cells was assessed by time-lapse microscopy. The growth of cells was followed by acquiring phase contrast and fluorescence pictures every 10 minutes for 4 hours, while cells were incubated at 37°C in a temperature-controlled setup (Cube and Box incubation system, Life Imaging Services, Reinach, Switzerland).

To follow microcolony growth on agarose pads, we used the same setup as described above, but this time inoculating pads with a highly diluted bacterial culture (dilution factor: $2.5*10^{-4}$). To induce iron limitation, we added 450 μM 2,2′-bipyridin to the agarose pad. We then identified independent fields of views, which contained single cells (max. 5 cells), and followed the gene expression of all cells in the growing microcolony over time. Phase contrast and fluorescence pictures

were acquired every 15 minutes for 5 hours. We obtained time-lapse data from 5 fields of views and gene expression data from approximately 1000 cells in total.

Analysis of microscopy pictures was conducted with ImageJ (freely available from http://rsbweb.nih.gov/ij/). Phase contrast pictures were used for masking cells. Cells were automatically thresholded, turned into masks, and bigger cell groups were split with the watershed filter. The position of the cell masks was stored with the 'analyzing particles' command, with a size-based selection (250-Infinity in pixel units). These masks were then checked manually by overlaying over the phase contrast pictures, and all false positives were removed. The masks were then overlaid over the fluorescence images. The background was removed by subtracting a fluorescent image without cells, specific for the time point measured, from the fluorescence image. If no such image was available (for data for Figure 5), the average intensity of two cell-free regions was used as background. Mean gfp-values were recorded for each cell, exported and analyzed in R3.1.1.

Mathematical model

The equation for the fitness effect of cooperation in the main text is:

$$ß(x, p, s) = p[B(sxp + (1 - s)x) - C(x)] + (1 - p)[B(sxp)] \quad (1)$$

where *p* is the proportion of compound producers in the group all producing quantity *x* of public good, and *s* is the shareability parameter, describing the proportion of compounds that are shared among clonemates. The first term in the equation represents the fitness of a producer of the public good. The benefit of this interaction is a function of the public good accessible to this individual, namely the products released and shared by others (*sxp*) as well as those released by itself but not shared with others *(1-s)x*. Producers also pay a cost for production, which is a function of their production *(x)*. The second term describes the fitness of a non-producer, which is the benefits obtained from others' secretions.

Results

Pyoverdine production entails diminishing costs and benefits

Given that *P. aeruginosa* requires a substantial assembly line for the synthesis and secretion of the iron-scavenging siderophore pyoverdine (biosynthesis occurs via nonribosomal peptide synthetases and involves at least 23 proteins (Visca et al. 2007)), we posit that this process could display the economies of scale, i.e. diminishing costs with increasing amount of pyoverdine production. To test this, we empirically quantified the cost function of pyoverdine production. For our experiments, we constructed the conditional pyoverdine mutant PAO1-*pvdSi*, in which the gene coding for the key pyoverdine synthesis regulator (iron starvation sigma factor PvdS) is under the control of an IPTG-inducible promoter. Inducing this strain across a range of IPTG concentrations in iron-replete media, where

pyoverdine is not needed, we found that the relative production costs significantly decelerate at higher pyoverdine production levels (Figure 1A) (quadratic fit significantly better than linear fit: $P < 0.0001$; $y = -2.75 \times 10^{-3} - 8.86 \times 10^{-11} x^2 + 3.49 \times 10^{-6} x$), supporting our hypothesis that pyoverdine biosynthesis follows the economies of scale. Additionally, we found that a low induction of PvdS actually resulted in a net benefit (i.e. negative costs in Figure 1A) under iron-replete conditions. This finding is compatible with the view that PvdS regulates, in addition to pyoverdine production, a number of other genes (Tiburzi et al. 2008), such that low PvdS expression can be beneficial even if pyoverdine is not needed for iron uptake.

Since optimality in compound production is determined by the interplay between costs and benefits (Dekel and Alon 2005; Cornforth et al. 2012), we also measured the benefit function of pyoverdine. In this experiment, we did not induce pyoverdine production with IPTG, but supplemented PAO1-*pvdSi* with different concentrations of purified pyoverdine. We found that benefits significantly diminished with increasing pyoverdine concentrations under conditions of strong iron limitation. This indicates that above a certain level of pyoverdine availability iron uptake can no further be increased, or alternatively, that iron is no longer the limiting resource. Our finding is in line with previous studies suggesting that diminishing returns are common for secreted metabolites (Foster 2004; Cornforth et al. 2012).

Modeling reveals that compound shareability determines whether individual or group optimality is favored

Based on our empirical findings, we used a simple mathematical model to explore how diminishing cost and benefit functions interact to shape bacterial fitness in a clonal group where individuals either all produce the same amount of compound (e.g. pyoverdine), or engage in specialization where only a fraction produces the compound. Furthermore, we investigated the effect of reduced shareability on the optimal expression pattern. We can express the net benefit to a bacterial group as

$$ß(x,p,s) = p[B(sxp + (1-s)x) - C(x)] + (1-p)[B(sxp)] \quad (1)$$

where B is a function representing the benefit of the compound, and C is the cost of compound production. p is the proportion of producers in the group, producing a quantity x (the other individuals produce none), and s is the shareability parameter, describing the proportion of compound that is shared among clonemates. We assume that an individual's production state (producer vs. non-producer) is non-heritable, and that individuals can change their state at any moment in time. To capture a monotonically increasing yet decelerating cost function we used $C(x) = g(1-e^{-hx})$, where g and h are scaling factors and x is the compound production level of producers. We used the same functional form for the benefit function, $B(x) = d(1-e^{-fx})$, but with d and f as scaling factors (Figure 2A). Important to note is that these functions were qualitatively inferred from the

decelerating shapes observed in our experiments (Figure 1), and not directly parameterized with data. A direct comparison of the cost and benefit functions is not possible because the unit of the x-axis differs for two curves (cumulative pyoverdine production in fluorescence unit vs. pyoverdine supplementation in μM).

Our model reveals that if compound shareability s is below a certain level and the amount of compound an individual cell can produce is constrained ($x \leq 1000$), the net benefit to a bacterial group β is maximized when all individuals engage in compound production (Figures 2B+D, Supplemental Information). In this case, we expect a uniform level of production across cells within a population. In contrast, if compound shareability is sufficiently high, then β is maximized by a division of labor, whereby a fraction of specialized individuals produces compounds for the entire group, while others completely refrain from production (Figures 2C+D).

Note that division of labor can also be adaptive with low shareability, but only if x is not constrained and is allowed to take on very large values (Supplementary Figure S1). In this case, massive compound production guarantees that still a significant absolute amount of metabolites reaches and benefits nonproducing neighboring cells, despite relative shareability being low. Here, we assume that such extreme production levels go beyond the biological capacity of an individual cell, and therefore focus on production levels for which $B(x) > C(x)$.

Though we used the arbitrary functions outlined above to demonstrate these effects, we emphasize that our findings apply more generally; namely that heterogeneity is advantageous whenever cost functions decelerate (see Supplemental Information for a general proof). Our modeling thus reveals that if shareability of secreted compounds exceeds a critical level, one may expect bacteria to evolve molecular mechanisms to restrict compound production to a fraction of the individuals in a clonal group.

Our model also shows that the adaptiveness of heterogeneity in the production of a secreted compound depends on a high reliability of compound sharing within the clonal bacterial collective. While sharing does not have to be complete (a fraction of the produced compound can preferentially accrue to the producer cell and division of labor could still evolve; see Figure 2D for $s<1$), there is a threshold of sharing below which heterogeneous expression is no longer optimal.

Analyses of pyoverdine expression indicate that production levels are optimized at the individual- and not the group-level

Our experiments showing that the cost function for pyoverdine production is decelerating, combined with our modeling insights allow us to make the following predictions: if – in the natural environment where *P. aeruginosa* has evolved – pyoverdine is sufficiently shared in clonal groups and mechanistic requirements are in place, we would expect that its production is restricted to only a fraction of

individuals. Conversely, if pyoverdine is not reliably shared, we expect that all individuals should produce similar amounts of pyoverdine. By analyzing production levels of individual cells we can thus gain insights into whether natural selection has predominantly acted on the level of the individual or the group with respect to pyoverdine production.

We measured pyoverdine production of individual cells in a growing population of *P. aeruginosa*. As a proxy for pyoverdine production we used the transcriptional reporter strain PAO1 *pvdA-gfp*. In this strain, the *egfp* gene, which encodes the green fluorescent protein, is under the control of the promoter of *pvdA*, one of the pyoverdine biosynthesis genes (Kaneko et al. 2007; Visca et al. 2007). In a first analysis of the reporter strain, we measured GFP expression of individual cells in a time-resolved manner using automated flow cytometry in environments differing in iron concentration. Iron availability alters the costs and benefits of pyoverdine production (Kümmerli et al. 2009b), which could potentially impact both individual- and group- level investment profiles. The data indeed show fine-tuned adjustments of mean pyoverdine expression levels in response to iron limitation and time (Figure 3A), indicating that *P. aeruginosa* adjusts pyoverdine expression to match prevailing levels of iron limitation. When looking at the individual-cell level, the distribution of GFP-signal intensity followed a unimodal distribution, with considerable variation around the mean but no clear signs of bimodality in *pvdA* expression across cells (Figure 3B).

We further assessed inter-individual variation in *pvdA* expression using single-cell microscopy, a method that yields higher resolution of gene expression differences, especially at low expression levels. In a first experiment, we analyzed the *pvdA* expression of single cells grown under well-mixed conditions, i.e. the same conditions used for the flow cytometry experiment. This analysis confirmed our observation that *pvdA* expression followed a unimodal and not a bimodal pattern at early time points of the experiment (Figure 4A). At later time points we observed the emergence of a subpopulation of individuals that did not express *pvdA*, but these cells neither grew nor expressed a second constitutively expressed control fluorophore (mCherry) (Figure 4B+C). This suggests that the cells not producing pyoverdine were generally inactive, a status possibly induced by the substrate shift from rich to minimal medium (van Heerden et al. 2014; Kotte et al. 2014).

The above experiments were carried out in well mixed environments, and thus explicitly rely on the assumption that bimodality should arise due to intrinsic gene expression noise. However, it might well be that bimodal expression of pyoverdine genes is triggered by variation in extracellular feedbacks, such as differences in local pyoverdine concentrations. Feedback variation should preferentially arise in spatially structured environments. To assess this possibility, we performed a second microscopy experiment, where we grew micro-colonies of cells on agarose pads and followed the *pvdA* expression of individual cells over time (similar to (Julou et al. 2013). This experiment also revealed a unimodal and not a bimodal

pyoverdine expression pattern (Figure 5). Taken together, our flow cytometry and microscopy data are consistent with the perspective that optimality in pyoverdine production in the natural environment is selected for at the level of the individual cell and not the group, even though secreted pyoverdine is highly shareable in laboratory settings (Meyer et al. 1997; De Vos et al. 2001; Griffin et al. 2004).

Discussion

We developed a novel concept showing how optimal production of a secreted compound can be established not only at the level of the individual cell, but also at the level of the clonal bacterial group. This group optimality can be achieved via a division of labor where a fraction of bacteria specializes in the production of the compound, while others do not produce it at all. We show that such specialization can evolve whenever compound production costs are diminishing and compounds are sufficiently shared within the clonal population. Our experiments on pyoverdine production in *P. aeruginosa* indeed revealed a diminishing cost function for this compound. This pattern might be common for many secreted secondary metabolites in bacteria, such as antibiotics, biosurfactants and siderophores, which are often assembled by modular polypeptides – nonribosomal peptide synthetases or polyketides (Donadio et al. 2007; Caboche et al. 2007; Miethke and Marahiel 2007; Weissman and Müller 2008), requiring large initial investments, but relatively minor production costs with larger outputs per cell.

The prerequisite we propose here, diminishing costs in the production of secreted bacterial compounds, could be a potentially widespread driver for the division of labor and an important addition to previously discussed scenarios that often require a trade-off between engaging in different types of tasks. In these examples, the basis of the evolution of division of labor lies in costs caused by task-switching or the incompatibility of tasks (Gavrilets 2010; Goldsby et al. 2012; Rueffler et al. 2012; Ispolatov et al. 2012), whereas we propose that division of labor could evolve solely due to diminishing production costs of a single trait. Moreover, microbial division of labor has also been associated with self-destructive behavior, where a fraction of cells expresses traits that lead to cell death, e.g. when cells trigger the inflammatory response in a host (Ackermann et al. 2008), or commit suicide to stop viral infections (Refardt et al. 2013). While division of labor is a necessity in the cases of task incompatibilities and self-destructive behavior to maintain a viable population, diminishing costs have subtler fitness consequences, and therefore can but must not stringently lead to the evolution of division of labor.

Despite the presence of diminishing costs in pyoverdine production, i.e. the mechanistic prerequisite being satisfied for division of labor to evolve, we found a unimodal and not a bimodal gene expression pattern across cells, suggesting the evolution of an individual- rather than a group-level optimum. As revealed by our model, one reason for a unimodal trait expression could be that pyoverdine shareability among clonemates is not high enough under natural conditions, such

that it pays off for each cell to produce its own immediate pool of pyoverdine instead of relying on pyoverdine produced by a clonemate that might or might not be present in the vicinity. We can think of at least three factors that could contribute to relatively low shareability of secreted compounds in natural environments. First, in certain environments, such as aquatic systems, bacterial cells are typically dispersed and occur at low density (Whitman et al. 1998). Experimental work on siderophores showed that compound sharing is significantly reduced under such conditions (Ross-Gillespie et al. 2009; Scholz and Greenberg 2015). If cells frequently switch between solitary and group living lifestyles heterogeneous expression of siderophores might not be the best strategy to satisfy a cell's iron requirement. Second, compound diffusivity likely represents a key factor determining compound sharing (Driscoll and Pepper 2010; Allen et al. 2013; Frank 2013). If compounds diffuse too readily then many of them will rapidly diffuse out of the range of non-producers and shareability is thus low (Kümmerli et al. 2014). In contrast, if compounds hardly diffuse away from producers then shareability among clonemates is also reduced (Kümmerli et al. 2009a; Julou et al. 2013). We would thus expect that an intermediate level of diffusion, where sharing is maximized and diffusion losses are low, should be most conducive to the evolution of division of labor. Whether and how frequently such conditions are met under natural conditions remains to be seen. Finally, bacterial groups might often not be clonal, in contrast to our model assumptions. Siderophore-producing bacteria could instead be surrounded by strains belonging to different species that neither

partake in compound production nor uptake, but which simply serve as physical obstacles, impeding efficient siderophore exchange among clonemates (Inglis et al. 2016). Alternatively, the community could include exploitative genotypes that use but never contribute to siderophore production. Such genotypes routinely arise and can come to dominate populations (Griffin et al. 2004; Cordero et al. 2012). In the presence of exploitative genotypes, producers may be induced to drive their own production up to maximal levels (Kümmerli et al. 2009b), presumably leaving little room for intraclonal division of labor to evolve.

In natural conditions, factors that favor or oppose the evolution of division of labor most likely fluctuate across time and space. Environmental fluctuations could either prevent specialization altogether, or could give rise to a facultative form of division of labor, where group-optimal behavior is expressed only if the required conditions of high shareability are met. While our experimental conditions, entailing both well-mixed and spatially structured environments, did not appear to have stimulated bimodal gene expression, we cannot exclude that a division of labor might be induced under different conditions. For instance, bimodal gene expression was shown to be associated with stressors (Cárcamo-Oyarce et al. 2015; Turnbull et al. 2016). It is certainly conceivable that cells can switch between different expression patterns that optimize benefit-cost ratios for groups versus individuals, and that these cellular decisions are based on cues or signals that

inform cells about changes in their environment (Lamont et al. 2002; Bassler and Losick 2006).

In this study, having first established that the principle of the economies of scale applies to microbial compound production, we have shown theoretically how this pattern of diminishing costs can promote the evolution of division of labor. However, we have also identified biological and physical constraints to the evolution of division of labor. This raises an important question: how frequently does selection act at the level of the group (as a functional unit) as opposed to the level of the individual (Michod 2006; Rueffler et al. 2012; Goldsby et al. 2012; West et al. 2015)? Given that microbes often form loose groups, where the reliability of compound sharing is probably low and conflicts among different genotypes are probably prevalent, we might expect that selection at the individual level has played a dominant role in the evolution of compound production in these organisms. However, more stable clonal cell aggregations (Wakano et al. 2009; Rossetti et al. 2010; Ratcliff et al. 2012; Olejarz and Nowak 2014) could promote a shift in the level of selection, from the individual to the group, potentially leading to a major transition in individuality (Pfeiffer and Bonhoeffer 2003; Michod 2007; West et al. 2015) including the evolution of division of labor in production of secreted compounds in bacterial groups.

Acknowledgements

We thank Frederik Hammes for support with flow cytometry. KTS, CB, and MA were supported by Eawag; KTS and MA were supported by ETH Zurich; ARG and RK were supported by the Swiss National Science foundation (grant no. PP00P3-139164); MW was supported by DAAG, and DMC was supported by a University of Edinburgh studentship.

References

Ackermann, M., B. Stecher, N. E. Freed, P. Songhet, W.-D. Hardt, and M. Doebeli. 2008. Self-destructive cooperation mediated by phenotypic noise. Nature 454:987–990.

Allen, B., J. Gore, and M. A. Nowak. 2013. Spatial dilemmas of diffusible public goods. eLife 2:1–11.

Bassler, B. L., and R. Losick. 2006. Bacterially speaking. Cell 125:237–246.

Bergmiller, T., R. Peña-Miller, A. Boehm, and M. Ackermann. 2011. Single-cell time-lapse analysis of depletion of the universally conserved essential protein YgjD. BMC Microbiology 11:118. BioMed Central Ltd.

Besmer, M. D., D. G. Weissbrodt, B. E. Kratochvil, J. A. Sigrist, M. S. Weyland, and F. Hammes. 2014. The feasibility of automated online flow cytometry for in-situ monitoring of microbial dynamics in aquatic ecosystems. Front Microbiol 5:265.

Caboche, S., M. Pupin, V. Leclere, A. Fontaine, P. Jacques, and G. Kucherov. 2007. NORINE: a database of nonribosomal peptides. Nucleic Acids Res 36:D326–D331.

Case, K., R. Fair, and S. M. Oster. 2011. Principles of Economics. 10 ed. Pearson Series in Economics.

Cárcamo-Oyarce, G., P. Lumjiaktase, R. Kümmerli, and L. Eberl. 2015. Quorum sensing triggers the stochastic escape of individual cells from Pseudomonas putida biofilms. Nat Comms 6:5945.

Choi, K.-H., and H. P. Schweizer. 2006. Mini-Tn7 insertion in bacteria with single attTn7 sites: example *Pseudomonas aeruginosa*. Nat Protoc 1:153–161.

Cordero, O. X., L.-A. Ventouras, E. F. Delong, and M. F. Polz. 2012. Public good dynamics drive evolution of iron acquisition strategies in natural bacterioplankton populations. Proc Natl Acad Sci U S A 109:20059–20064.

Cornforth, D. M., D. J. T. Sumpter, S. P. Brown, and Å. Brännström. 2012. Synergy and Group Size in Microbial Cooperation. Am. Nat 180:296–305.

De Vos, D., M. de Chial, C. Cochez, S. Jansen, B. Tummler, J. M. Meyer, and P. Cornelis. 2001. Study of pyoverdine type and production by Pseudomonas aeruginosa isolated from cystic fibrosis patients: prevalence of type II pyoverdine isolates and accumulation of pyoverdine-negative mutations. Archives of Microbiology 175:384–388.

Dekel, E., and U. Alon. 2005. Optimality and evolutionary tuning of the expression level of a protein. Nature 436:588–592.

Diard, M., V. Garcia, L. Maier, M. N. P. Remus-Emsermann, R. R. Regoes, M. Ackermann, and W.-D. Hardt. 2013. Stabilization of cooperative virulence by the expression of an avirulent phenotype. Nature 494:353–356. Nature Publishing Group.

Diggle, S. P., A. S. Griffin, G. S. Campbell, and S. A. West. 2007. Cooperation and conflict in quorum-sensing bacterial populations. Nature 450:411–414.

Donadio, S., P. Monciardini, and M. Sosio. 2007. Polyketide synthases and nonribosomal peptide synthetases: the emerging view from bacterial genomics. Nat. Prod. Rep 24:1073.

Driscoll, W. W., and J. W. Pepper. 2010. Theory for the evolution of diffusible external goods. Evolution 64:2682–2687.

Dubnau, D., and R. Losick. 2006. Bistability in bacteria. Mol Microbiol 61:564–572.

Dumas, Z., A. Ross-Gillespie, and R. Kümmerli. 2013. Switching between apparently redundant iron-uptake mechanisms benefits bacteria in changeable environments. Proc R Soc Lond [Biol] 280:20131055–20131055. The Royal Society.

Eames, M., and T. Kortemme. 2012. Cost-benefit tradeoffs in engineered lac operons. Science 336:911–915. American Association for the Advancement of Science.

Foster, K. R. 2004. Diminishing returns in social evolution: the not-so-tragic commons. J. Evol. Biol. 17:1058–1072.

Frank, S. A. 2013. Evolution of Robustness and Cellular Stochasticity of Gene Expression. PLoS One 11:e1001578. Public Library of Science.

Gavrilets, S. 2010. Rapid Transition towards the Division of Labor via Evolution of Developmental Plasticity. PLoS Comput. Biol. 6:e1000805.

Ghysels, B., B. T. M. Dieu, S. A. Beatson, J.-P. Pirnay, U. A. Ochsner, M. L. Vasil, and P. Cornelis. 2004. FpvB, an alternative type I ferripyoverdine receptor of *Pseudomonas aeruginosa*. Microbiology (Reading, Engl.) 150:1671–1680.

Goldsby, H. J., A. Dornhaus, B. Kerr, and C. Ofria. 2012. Task-switching costs promote the evolution of division of labor and shifts in individuality. Proc Natl Acad Sci U S A 109:13686–13691. National Acad Sciences.

Griffin, A. S., S. A. West, and A. Buckling. 2004. Cooperation and competition in pathogenic bacteria. Nature 430:1024–1027.

Inglis, R. F., J. M. Biernaskie, A. Gardner, and R. Kümmerli. 2016. Presence of a loner strain maintains cooperation and diversity in well-mixed bacterial communities. Proc R Soc Lond [Biol] 283.

Ispolatov, I., M. Ackermann, and M. Doebeli. 2012. Division of labour and the evolution of multicellularity. Proc R Soc Lond [Biol] 279:1768–1776.

Julou, T., T. Mora, L. Guillon, V. Croquette, I. J. Schalk, D. Bensimon, and N. Desprat. 2013. Cell-cell contacts confine public goods diffusion inside *Pseudomonas aeruginosa* clonal microcolonies. Proc Natl Acad Sci U S A 110:12577–12582.

Kahm, M., G. Hasenbrink, H. Lichtenberg-Fraté, J. Ludwig, and M. Kschischo. 2010. grofit : Fitting Biological Growth Curves with R. J STAT SOFTW 33.

Kaneko, Y., M. Thoendel, O. Olakanmi, B. E. Britigan, and P. K. Singh. 2007. The transition metal gallium disrupts *Pseudomonas aeruginosa* iron metabolism and has antimicrobial and antibiofilm activity. J Clin Invest 117:877–888.

Kotte, O., B. Volkmer, J. L. Radzikowski, and M. Heinemann. 2014. Phenotypic bistability in *Escherichia coli*'s central carbon metabolism. Mol Syst Bio 10:736.

Kümmerli, R., A. S. Griffin, S. A. West, A. Buckling, and F. Harrison. 2009a. Viscous medium promotes cooperation in the pathogenic bacterium *Pseudomonas aeruginosa*. Proceedings of the Royal Society B: Biological Sciences 276:3531–3538.

Kümmerli, R., K. T. Schiessl, T. Waldvogel, K. McNeill, and M. Ackermann. 2014. Habitat structure and the evolution of diffusible siderophores in bacteria. Ecol Lett 17:1536–1544.

Kümmerli, R., N. Jiricny, L. S. Clarke, S. A. West, and A. S. Griffin. 2009b. Phenotypic plasticity of a cooperative behaviour in bacteria. J Evol Biol 22:589–598.

Lambertsen, L., C. Sternberg, and S. Molin. 2004. Mini-Tn7 transposons for site-specific tagging of bacteria with fluorescent proteins. Environ Microbiol 6:726–732.

Lamont, I. L., P. A. Beare, U. Ochsner, A. I. Vasil, and M. L. Vasil. 2002. Siderophore-mediated signaling regulates virulence factor production in Pseudomonas aeruginosa. Proc Natl Acad Sci U S A 99:7072–7077. National Acad Sciences.

Maechler, M., and D. Ringach. 2013. diptest: Hartigan's dip test statistic for unimodality corrected code. R package version 0.75-5.

Meyer, J.-M., A. Stintzi, D. De Vos, P. Cornelis, R. Tappe, and H. Budzikiewicz. 1997. Use of siderophores to type pseudomonads: the three *Pseudomonas aeruginosa* pyoverdine systems. Microbiology 35–43.

Michod, R. E. 2007. Evolution of individuality during the transition from unicellular to multicellular life. Proc Natl Acad Sci U S A 104 Suppl 1:8613–8618. National Acad Sciences.

Michod, R. E. 2006. The group covariance effect and fitness trade-offs during evolutionary transitions in individuality. Proc Natl Acad Sci U S A 103:9113–9117.

Miethke, M., and M. A. Marahiel. 2007. Siderophore-based iron acquisition and pathogen control. Microbiol Mol Biol Rev 71:413–451.

Olejarz, J. W., and M. A. Nowak. 2014. Evolution of staying together in the context of diffusible public goods. J Theor Biol 360:1–12. Elsevier.

Pfeiffer, T., and S. Bonhoeffer. 2003. An evolutionary scenario for the transition to undifferentiated multicellularity. Proc Natl Acad Sci U S A 100:1095–1098. National Acad Sciences.

Poelwijk, F. J., P. D. Heyning, M. G. de Vos, D. J. Kiviet, and S. J. Tans. 2011. Optimality and evolution of transcriptionally regulated gene expression. BMC Syst. Biol 5:128. BioMed Central Ltd.

Price, M. N., A. M. Deutschbauer, J. M. Skerker, K. M. Wetmore, T. Ruths, J. S. Mar, J. V. Kuehl, W. Shao, and A. P. Arkin. 2013. Indirect and suboptimal control of gene expression is widespread in bacteria. Mol Syst Bio 9:660–660. EMBO Press.

Ratcliff, W. C., R. F. Denison, M. Borrello, and M. Travisano. 2012. Experimental evolution of multicellularity. Proc Natl Acad Sci U S A 109:1595–1600. National Acad Sciences.

Refardt, D., T. Bergmiller, and R. Kümmerli. 2013. Altruism can evolve when relatedness is low: evidence from bacteria committing suicide upon phage infection. Proc R Soc Lond [Biol] 280:20123035–20123035. The Royal Society.

Ross-Gillespie, A., A. Gardner, A. Buckling, S. A. West, and A. S. Griffin. 2009. Density dependence and cooperation: theory and a test with bacteria. Evolution 63:2315–2325.

Rossetti, V., B. E. Schirrmeister, M. V. Bernasconi, and H. C. Bagheri. 2010. The evolutionary path to terminal differentiation and division of labor in cyanobacteria. J Theor Biol 262:23–34. Elsevier.

Rueffler, C., J. Hermisson, and G. P. Wagner. 2012. Evolution of functional specialization and division of labor. Proc Natl Acad Sci U S A 109:E326–35.

Sanchez, A., and J. Gore. 2013. Feedback between population and evolutionary dynamics determines the fate of social microbial populations. PLoS Biol, doi: 10.1371/journal.pbio.1001547.s006.

Scholz, R. L., and E. P. Greenberg. 2015. Sociality in *Escherichia coli*: Enterochelin Is a Private Good at Low Cell Density and Can Be Shared at High Cell Density. J Bacteriol 197:2122–2128. American Society for Microbiology.

Shachrai, I., A. Zaslaver, U. Alon, and E. Dekel. 2010. Cost of unneeded proteins in *E. coli* is reduced after several generations in exponential growth. Mol Cell 38:758–767.

Tiburzi, F., F. Imperi, and P. Visca. 2008. Intracellular levels and activity of PvdS, the major iron starvation sigma factor of *Pseudomonas aeruginosa*. Mol Microbiol 67:213–227.

Turnbull, L., M. Toyofuku, A. L. Hynen, M. Kurosawa, G. Pessi, N. K. Petty, S. R. Osvath, G. Cárcamo-Oyarce, E. S. Gloag, R. Shimoni, U. Omasits, S. Ito, X. Yap, L. G. Monahan, R. Cavaliere, C. H. Ahrens, I. G. Charles, N. Nomura, L. Eberl, and C. B. Whitchurch. 2016. Explosive cell lysis as a mechanism for the biogenesis of bacterial membrane vesicles and biofilms. Nat Comms 7:11220.

van Gestel, J., F. J. Weissing, O. P. Kuipers, and A. T. Kovács. 2014. Density of founder cells affects spatial pattern formation and cooperation in *Bacillus subtilis* biofilms. ISME J 8:2069–2079.

van Gestel, J., H. Vlamakis, and R. Kolter. 2015. From cell differentiation to cell collectives: *Bacillus subtilis* uses division of labor to migrate. PLoS Biol 13.

van Heerden, J. H., M. T. Wortel, F. J. Bruggeman, J. J. Heijnen, Y. J. M. Bollen, R. Planqué, J. Hulshof, T. G. O'Toole, S. A. Wahl, and B. Teusink. 2014. Lost in transition: start-up of glycolysis yields subpopulations of nongrowing cells. Science 343:1245114. American Association for the Advancement of Science.

Veening, J.-W., W. K. Smits, and O. P. Kuipers. 2008. Bistability, Epigenetics, and Bet-Hedging in Bacteria. Annu. Rev. Microbiol. 62:193–210.

Visca, P., F. Imperi, and I. L. Lamont. 2007. Pyoverdine siderophores: from biogenesis to biosignificance. Trends Microbiol 15:22–30.

Wakano, J. Y., M. A. Nowak, and C. Hauert. 2009. Spatial dynamics of ecological public goods. Proc Natl Acad Sci U S A 106:7910–7914. National Acad Sciences.

Weissman, K. J., and R. Müller. 2008. Protein–Protein Interactions in Multienzyme Megasynthetases. ChemBioChem 9:826–848.

West, S. A., and G. A. Cooper. 2016. Division of labour in microorganisms: an evolutionary perspective. Nature Rev. Microbio, doi: 10.1038/nrmicro.2016.111.

West, S. A., R. M. Fisher, A. Gardner, and E. T. Kiers. 2015. Major evolutionary transitions in individuality. Proc Natl Acad Sci U S A 112:10112–10119. National Acad Sciences.

Whitman, W. B., D. C. Coleman, and W. J. Wiebe. 1998. Prokaryotes: the unseen majority. Proc Natl Acad Sci U S A 95:6578–6583.

Xavier, J. B., W. Kim, and K. R. Foster. 2011. A molecular mechanism that stabilizes cooperative secretions in *Pseudomonas aeruginosa*. Mol Microbiol 79:166–179.

Figure legends

Figure 1. Diminishing costs and benefits of pyoverdine production. In (A), we induced pyoverdine production in strain PAO1-*pvdSi* by the addition of increasing concentrations of IPTG under conditions where it is not required for growth. We measured the decrease in maximal growth rate (relative to IPTG-free conditions) as a function of observed pyoverdine output (i.e. the integral of pyoverdine-associated fluorescence up to the point of peak production, which is a linear predictor of absolute pyoverdine content as previously shown by (Dumas et al. 2013). The relationship between the variables was significantly better described by a quadratic rather than a linear fit ($P < 0.0001$), indicating diminishing costs for pyoverdine production. Points and error bars show means and standard errors across n = 8 replicates. In (B), purified pyoverdine was added to cultures of non-induced PAO1-*pvdSi* under iron-depleted conditions. We measured the increase in maximal growth rate (relative to unsupplemented conditions) as a function of pyoverdine supplementation. Here a power function explained more variance than either a linear or a quadratic fit [$\log(y) = -6.15 + 0.40 \times \log(x)$]. Points and error bars show mean and standard errors across n = 6 replicates.

Figure 2. The evolution of group optimality depends on the shareability of compounds. (A) The exponentially decelerating cost (red) and benefit (blue) functions used for our exemplary model (see Supplementary material for a general

proof). (B) Under conditions where compound shareability is low ($s = 0.05$), the net benefit to the bacterial group β decreases with lower proportion of producers (p, number above line), and optimality is reached when every single cell produces the same amount of the compound. Net benefit functions are green (for $p = 1$) or grey (for $p < 1$). (C) Under conditions where compound shareability is high ($s = 1$), the net benefit to the group β increases when only a fraction of cells invests in compound production. Here, selection favors a group optimum, where a relatively small fraction of individuals produces the compound for the entire collective. (D) Contour plot depicting how the net benefit to the group β (with maximizing x, the production level per producer) varies as a function of p and s (assuming $x \leq 1000$). For all panels, we used the scaling factors $d = 25$; $f = 0.004$; $g = 30$; $h = 0.0015$.

Figure 3. Tuning of pyoverdine expression in response to iron availability and time. (A) Population-level median GFP expression over time for the *pvdA-gfp* reporter (red lines) and the constitutive *gfp* reporter (grey lines) under different iron supplementation regimes (circles = 0 μM iron added, squares = 5 μM iron added, diamonds = 20 μM iron added). The blue line depicts background fluorescence signal of the wildtype PAO1 strain without reporter. (B) shows the distributions of individual-level GFP expression of the *pvdA-gfp* reporter (red), the constitutive *gfp* reporter (grey), and the wildtype control (blue) for the 0 μM and 5 μM iron supplementation regimes, respectively. While the data indicate that the absolute level of pyoverdine expression is extremely fine-tuned in response to iron

availability and over time, in all cases the observed values are clearly unimodally distributed.

Figure 4. Microscopy reveals a unimodal *pvdA* expression among growing cells. (A) Histograms show distributions of individual-level GFP expression of the *pvdA-gfp* reporter (red), the constitutive *gfp* reporter (grey), and the wildtype strain without *gfp* reporter (blue) over time. Microscopy pictures show representative snapshots of the PAO1*pvdA-gfp* strain (brightness and contrast were adjusted manually). Data reveal a significant increase in bimodality in pyoverdine expression over time (linear increase of Hartigan's *Dn*, diptest for bimodality (Maechler and Ringach 2013), for the *pvdA-gfp* reporter: $t_{66} = 2.85$, $p = 0.006$, but neither for the constitutive *gfp* reporter control: $t_{66} = 1.16$, $p = 0.249$, nor for the wildtype strain without *gfp*: $t_{66} = -0.94$, $p = 0.352$). However, (B) fluorescence from expression of a constitutive *mcherry* control marker served as a significant linear predictor of fluorescence from expression of pyoverdine (*pvdA-gfp*) both for growing (filled circles) and non-growing cells (empty squares). This suggests that pyoverdine expression levels are linked to the overall cellular gene expression activity. (C) A cell's pyoverdine (*pvdA-gfp*) expression was significantly predictive, in a logistic regression, of its growth status: dividing cells (circles; ≥ 2 divisions observed within four hours) showed significantly higher *pvdA-gfp* expression than non-dividing cells (squares), indicating that bimodality in pyoverdine expression at the whole population level is mainly driven by bistability in the growth status of

cells. Indeed, when non-dividing cells are excluded, we no longer see bimodality in *pvdA*-*gfp* expression ($Dn = 0.024$, $p = 0.485$).

Figure 5. The expression of *pvdA* is also unimodal when cells grow in a spatially structured environment. Histograms show distributions of individual-level GFP expression of the *pvdA*-*gfp* reporter (red) over time. Cells were inoculated at low density onto agarose pads and their growth and individual *pvdA* expression was tracked over time using automated time-lapse microscopy. Data show gene expression profiles in 30-minutes intervals, starting from 90 minutes after the start of the experiment.

Figures

Figure 1

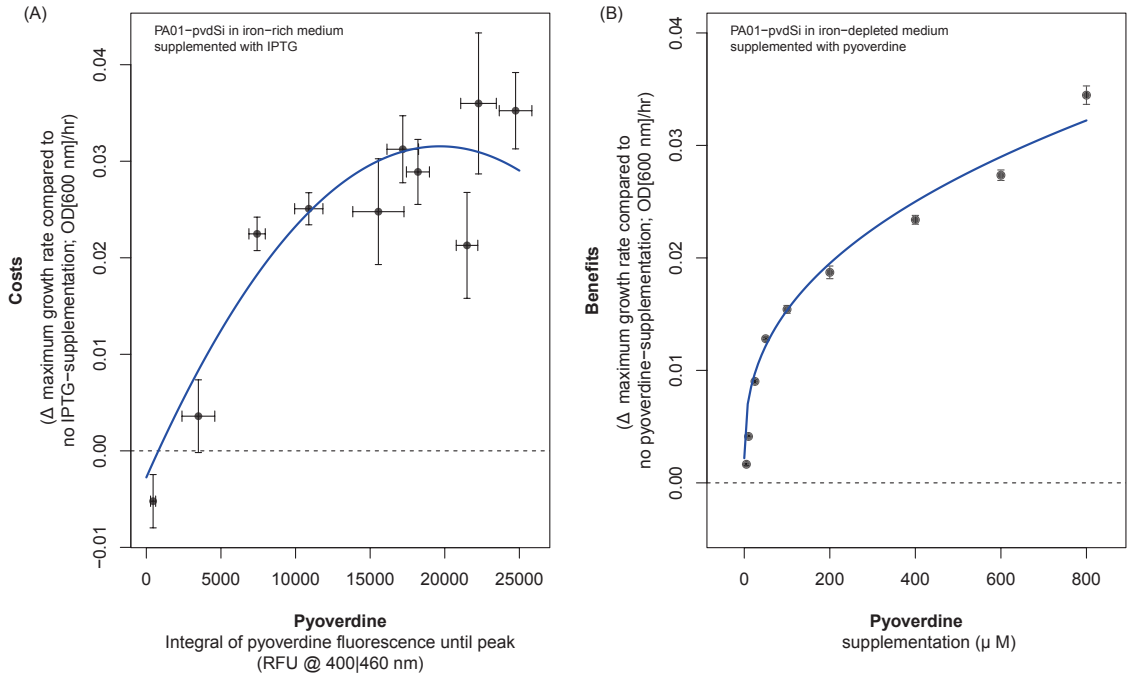

Figure 2

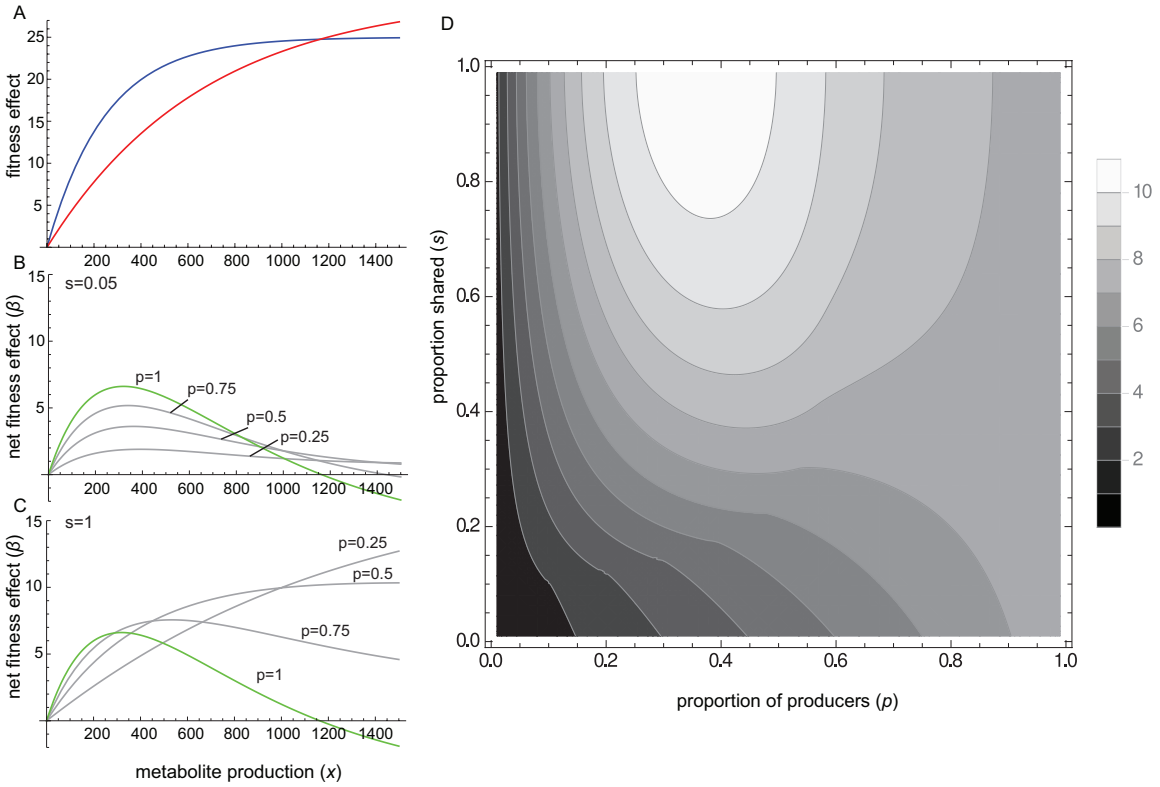
A
fitness effect
B
s=0.05
net fitness effect (β)
p=1
p=0.75
p=0.5
p=0.25
C
s=1
net fitness effect (β)
p=0.25
p=0.5
p=0.75
p=1
metabolite production (x)
D
proportion shared (s)
proportion of producers (p)

Figure 3

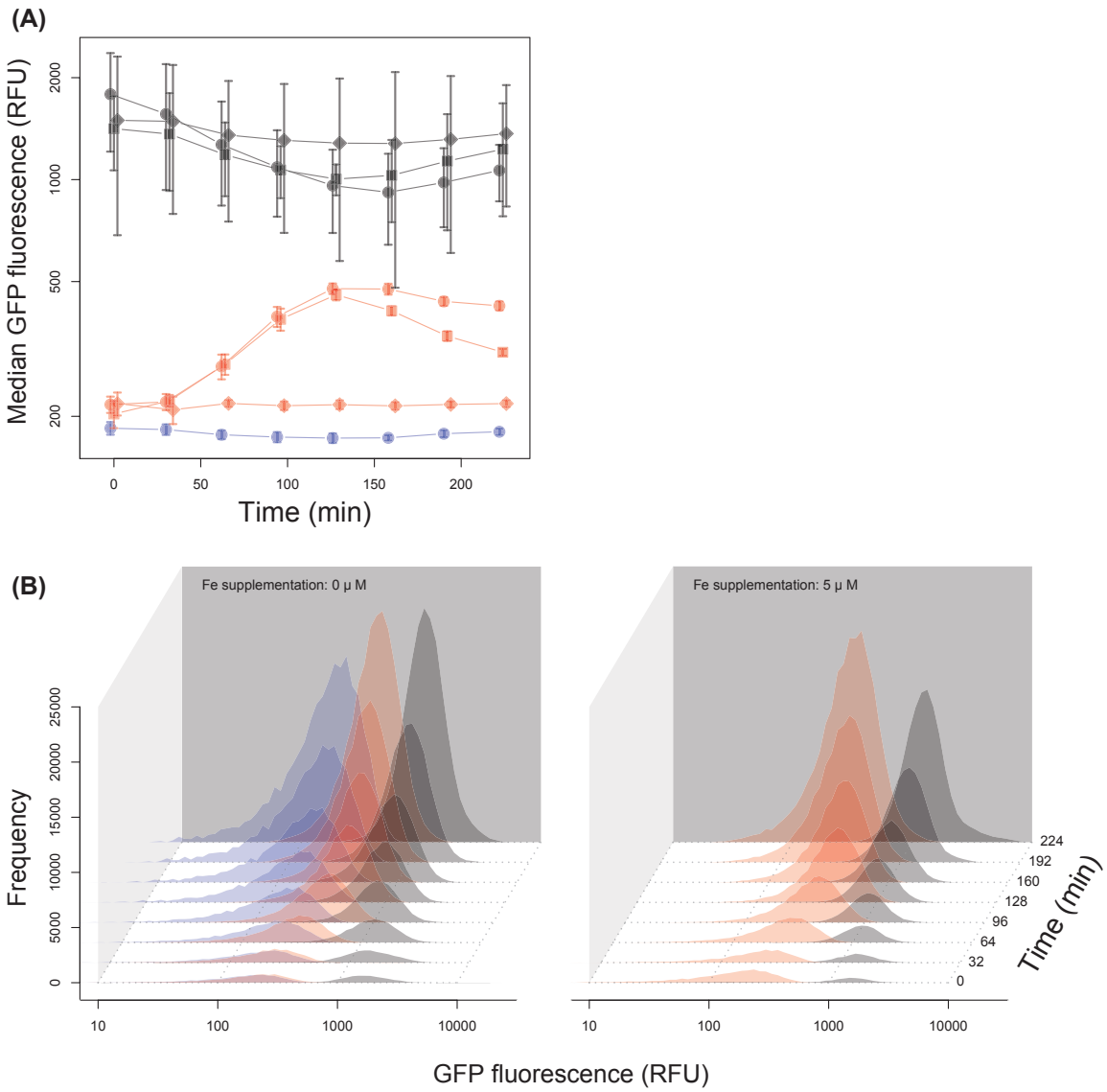
(A)
Median GFP fluorescence (RFU)
2000
1000
500
200
0
50
100
150
200
Time (min)
(B)
Fe supplementation: 0 μ M
Fe supplementation: 5 μ M
Frequency
25000
20000
15000
10000
5000
0
10
100
1000
10000
224
192
160
128
96
64
32
0
Time (min)
GFP fluorescence (RFU)

Figure 4

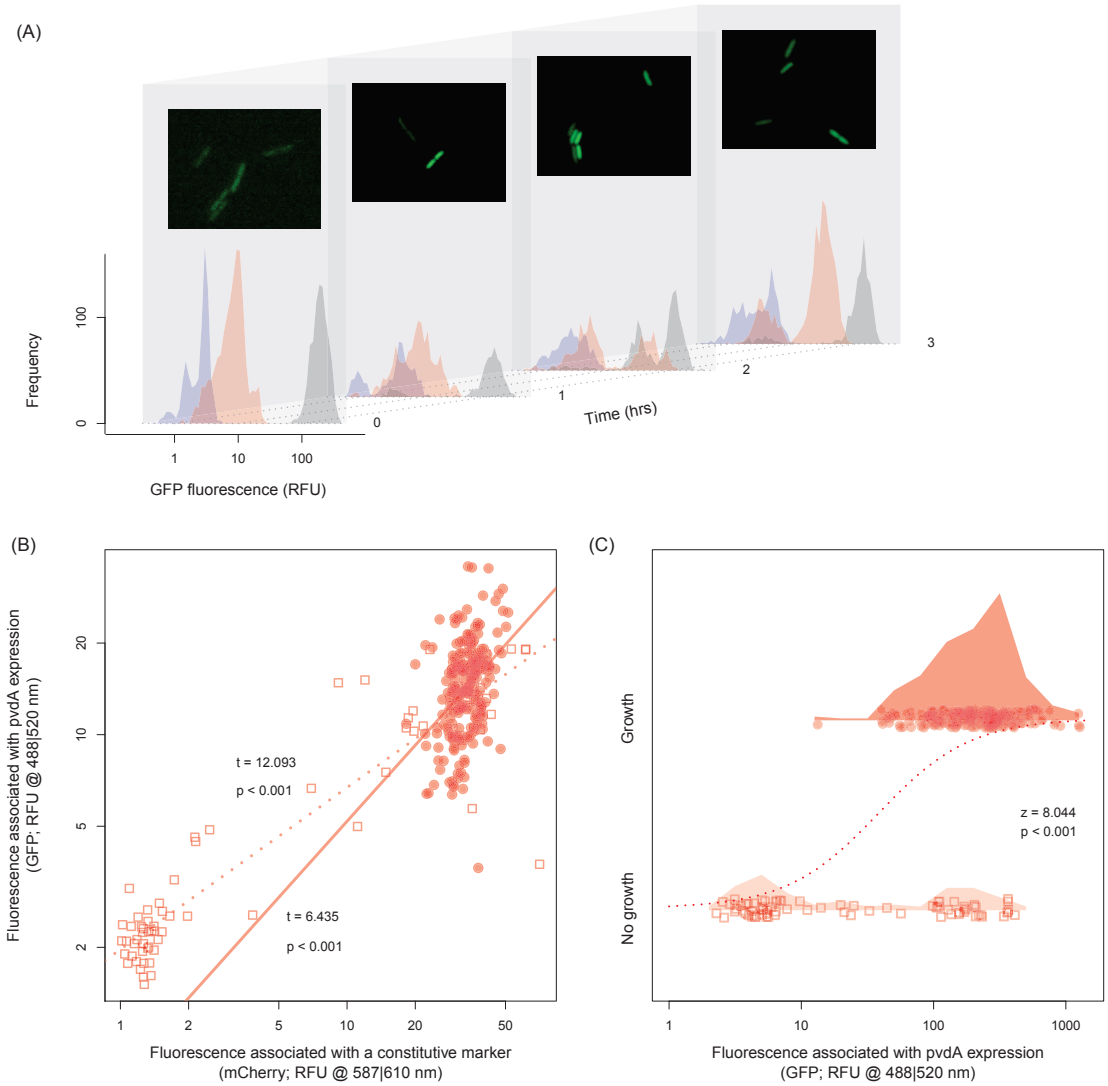
(A)
Frequency
100
0
1
10
100
GFP fluorescence (RFU)
0
1
2
3
Time (hrs)
(B)
Fluorescence associated with pvdA expression
(GFP; RFU @ 488|520 nm)
20
10
5
2
t = 12.093
p < 0.001
t = 6.435
p < 0.001
1
2
5
10
20
50
Fluorescence associated with a constitutive marker
(mCherry; RFU @ 587|610 nm)
(C)
Growth
No growth
z = 8.044
p < 0.001
1
10
100
1000
Fluorescence associated with pvdA expression
(GFP; RFU @ 488|520 nm)

Figure 5

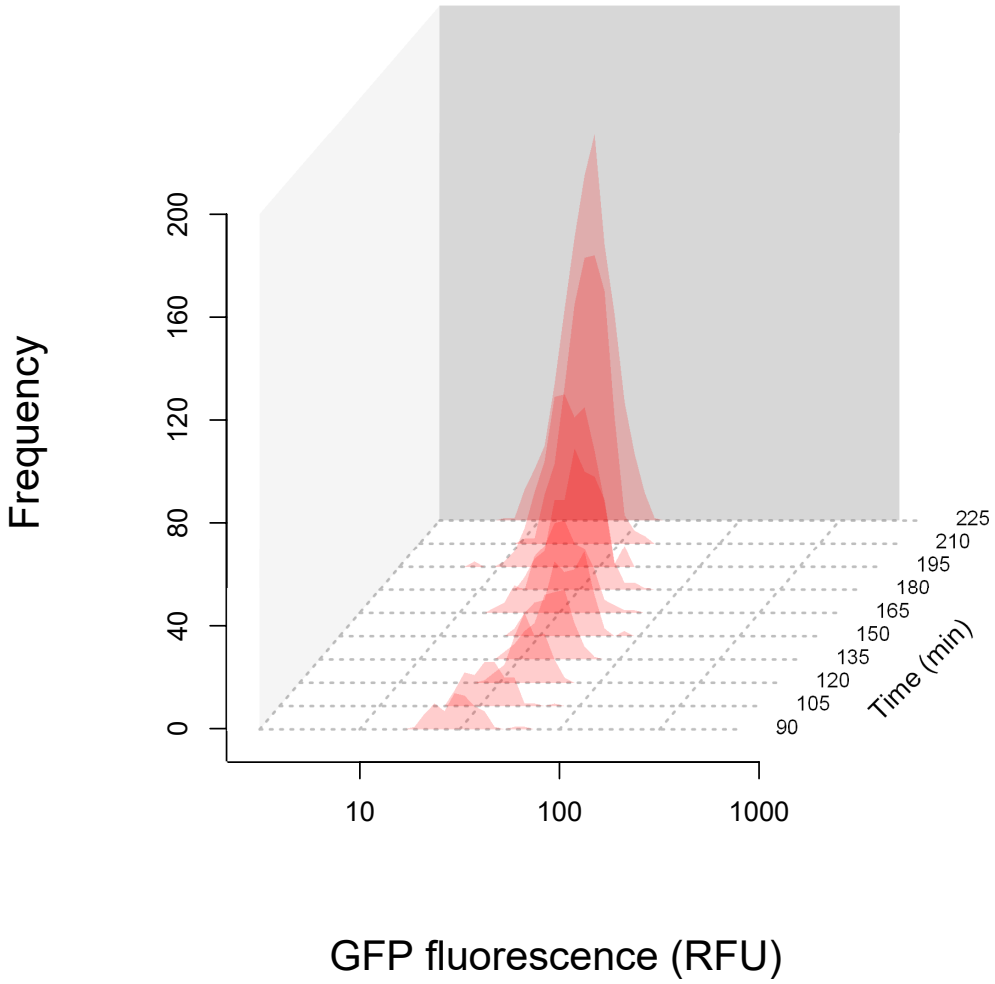
Frequency
0
40
80
120
160
200
10
100
1000
GFP fluorescence (RFU)
Time (min)
90
105
120
135
150
165
180
195
210
225

Supplementary Material

Division of labor is optimal for any decelerating cost function if shareability is sufficiently high

Though the main text assumes specific cost and benefit functions, the advantage of division of labor holds in the model from the main text as long as the cost function is decelerating and shareability is sufficiently high.

Theorem 1: Assuming the fitness function in the main text, for any differentiable benefit and cost functions (B(x) and C(x) respectively), with $x \in [0, \infty)$, that cross through the origin [$C(0) = B(0) = 0$] where the cost function has negative concavity [$C''(x) < 0$ for all x], there exists a value $0 \leq s^* < 1$ such that for any shareability constant $s > s^*$, fitness decreases as *p* decreases if *xp* is held constant (or equivalently, fitness increases as *x* increases, if *xp* is constant). In other words, assuming total production (xp) is constant, at a sufficiently high shareability level, fitness increases as the proportion of non-producers does.

Proof:

First we show that the fitness function from the main text increases with *x* for the case where $s = 1$. If we fix xp (letting constant $q = xp$), we can express the fitness function as

$$\beta_2(x,s) = \frac{q}{x}\big(B(qs + (1-s)x) - C(x)\big) + \left(1 - \frac{q}{x}\right)B(qs) \qquad (2)$$

The derivative of this function with respect to *x* ($\frac{d}{dx}\beta_2(x,s)$) simplifies to $p\left(C(x) - xC'(x)\right)/x$ for the case where $s = 1$. Because p/x is positive, if $C(x) - xC'(x)$ is positive for all *x*, then the whole derivative is positive. Since *C* has negative concavity and goes through the origin, the line tangent to $C(x)$ at any fixed x_1 crosses the x-axis to the left of the origin. Call this tangent line $L(x) = xC'(x_1) + b$ (where $b > 0$). So $L(x_1) = C(x_1) = xC'(x_1) + b$. Therefore $C(x_1) > xC'(x_1)$, and more generally $C(x) > xC'(x)$ over the interval.

This means when $s = 1$, $\frac{d}{dx}\beta_2(x,s) > 0$. Because $\frac{d}{dx}\beta_2(x,s)$ is continuous, there exists a $0 \leq s^* < 1$ such that for all $s \in [s^*, 1]$, $\frac{d}{dx}\beta_2(x,s) > 0$. Or, in words, when the shareability constant (*s*) is sufficiently high (with no restrictions on *p* or *x*), fitness is maximized at arbitrarily low *p* and high *x*. ▌

In the specific model in the main text, the production, *x*, has a maximum value at which production cannot be increased further. So rather than the optimal value of *x* for any particular overall production level (*xp*) being arbitrarily high when shareability is sufficiently high, the optimal value is simply the maximum allowable value.

Division of labor is not generally optimal for a decelerating cost function if shareability is sufficiently low

On the other hand, if public goods are *not* freely shared with others, then division of labor is not generally beneficial. At an extreme, when there is no sharing ($s = 0$), then $ß(x, p) = p[B(x) - C(x)]$; and so fitness is maximized at $p = 1$ with some corresponding *x*. With an additional assumption that $C(x) - xC'(x) > B(x) - xB'(x)$ in some interval $[a, b]$ then the maximal fitness for a given *xp* value (with *p* in the interval $[a, b]$) occurs at *p*=1 for any shareability level below a cutoff.

Theorem 2: Suppose there are differentiable benefit and cost functions (B(x) and C(x) respectively), with $x \in [0, \infty)$, that cross through the origin [$C(0) = B(0) = 0$]. If $C(x) - xC'(x) > B(x) - xB'(x)$ over some interval $[a, b]$ then there exists a value $0 \leq s^* < 1$ such that for any shareability constant $s < s^*$, the maximal fitness for a given *xp* (with *xp* in the interval $[a, b]$) occurs at *p*=1.

The derivative of the function β_2 with respect to *x* ($\frac{d}{dx}\beta_2(x, s)$) simplifies to $p\left[\left(xB'(x) - B(x)\right) - \left(xC'(x) - C(x)\right)\right]/x$ for the case where $s = 0$.

Because p/x is positive and $\left(xB'(x) - B(x)\right) - \left(xC'(x) - C(x)\right)$ is negative in the interval $[a, b]$, then the whole derivative is negative. This means when $s = 0$, $\frac{d}{dx}\beta_2(x, s) < 0$ in this interval. Because $\frac{d}{dx}\beta_2(x, s)$ is continuous, there exists a $0 \leq s^* < 1$ such that for all $s \in [0, s^*]$, $\frac{d}{dx}\beta_2(x, s) < 0$ in the interval $[a, b]$. So when the

shareability constant (*s*) is sufficiently low, for a given value of *xp*, fitness is maximized at *p*=1.

In the example in the main text, $C(x) - xC'(x) > B(x) - xB'(x)$ for *x* values high enough to optimize fitness, so there is typically a threshold below which heterogeneity is disfavored in this example.

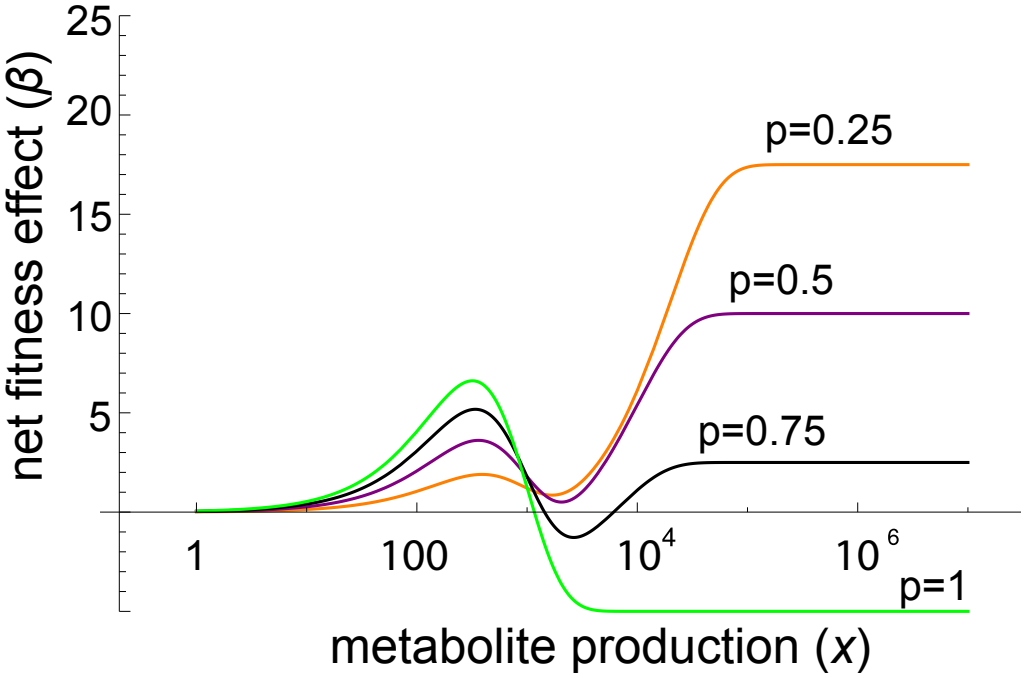

Figure S1: The fitness effect of very high metabolite production levels with low shareability (s=0.05). Though at the lower range of production, more producers lead to higher fitness (as shown in Fig. 2B), at higher levels of production this trend reverses. Even with very limited shareability, the lowest producer proportion (here p=0.25) fares better than all the others at very high production levels. The parameters are the same as in Figure 2 (d = 25; f = 0.004; g = 30; h = 0.0015).